JACS
JOURNAL OF THE AMERICAN CHEMICAL SOCIETY
Communication
pubs.acs.org/JACS

Sizing by Weighing: Characterizing Sizes of Ultrasmall-Sized Iron Oxide Nanocrystals Using MALDI-TOF Mass Spectrometry

Byung Hyo Kim,[†] Kwangsoo Shin,[†] Soon Gu Kwon,[†] Youngjin Jang,[†] Hyun-Seok Lee,[‡] Hyunjae Lee,[†] Samuel Woojoo Jun,[†] Jisoo Lee,[†] Sang Yun Han,[§] Yong-Hyeon Yim,[‡] Dae-Hyeong Kim,[†] and Taeghwan Hyeon*,[†]

[†]Center for Nanoparticle Research, Institute for Basic Science, and School of Chemical and Biological Engineering, Seoul National University, Seoul 151-742, Korea

[‡]Center for Analytical Chemistry, Korea Research Institute of Standards and Science, Daejeon 305-340, Korea

[§]Center for Nano-Bio Technology, Korea Research Institute of Standards and Science, Daejeon 305-340, Korea

Supporting Information

ABSTRACT: We present a rapid and reliable method for determining the sizes and size distributions of <5 nm-sized iron oxide nanocrystals (NCs) using matrix-assisted laser desorption/ionization time of flight (MALDI-TOF) mass spectrometry (MS). MS data were readily converted to size information using a simple equation. The size distribution obtained from the mass spectrum is well-matched with the data from transmission electron microscopy, which requires long and tedious analysis work. The size distribution obtained from the mass spectrum is highly resolved and can detect size differences of only a few angstroms. We used this MS-based technique to investigate the formation of iron oxide NCs, which is not easy to monitor with other methods. From ex situ measurements, we observed the transition from molecular precursors to clusters and then finally to NCs.

Precise measurement of the sizes and size distributions of ultrasmall-sized nanocrystals (NCs) is very important for both fundamental property characterizations and technological applications because NCs exhibit characteristic size-dependent electrical, optical, magnetic, and chemical properties.[1] Transmission electron microscopy (TEM) is one of the most popularly employed techniques for measuring the size of NCs. However, obtaining TEM images and subsequent extraction of size information is a laborious and time-consuming process. Furthermore, it is very difficult to obtain high-quality TEM images of NCs with sizes of <2 nm, and it is nearly impossible to get TEM images of clusters with sizes of <1 nm.[2] Although fitting of the line broadening of powder X-ray diffraction (XRD) patterns to the Scherrer equation has been used to calculate NC sizes, the acquired size data are inherently inaccurate, and it is therefore impossible to obtain size distribution data.[3a] Other size characterization methods, including dynamic light scattering (DLS) and small-angle X-ray scattering (SAXS), cannot accurately measure small-sized nanoparticles with diameters of <5 nm.[3b,c]

Iron oxide NCs exhibit very interesting size-dependent magnetic properties, and uniform-sized iron oxide NCs with controlled sizes have recently been intensively investigated as magnetic resonance imaging (MRI) contrast agents.[4,5] For example, superparamagnetic iron oxide NCs with sizes of 5−20 nm have been used as T_2 MRI contrast agents for diagnosis of cancers,[4d] and 50 nm-sized ferrimagnetic iron oxide NCs were employed as MRI contrast agents for single cells and transplanted pancreas islet cells.[4e] Ultrasmall iron oxide NCs with sizes in the range 1−5 nm, comprising 100 to 10,000 atoms, exhibit properties intermediate between paramagnetic iron−oxo clusters and superparamagnetic iron oxide NCs.[5,6] Recently, uniform 3 nm-sized iron oxide NCs were developed as a highly sensitive T_1 MRI contrast agent for imaging of blood vessels with sizes of <0.2 mm.[5]

Understanding NC formation mechanisms, including the nucleation and growth processes, is very important for the development of new synthetic methods to obtain NCs with desired characteristics.[7−9] For these mechanistic studies, the collection of size distribution data is critical. UV−vis absorption and photoluminescence spectroscopies have been successfully used to elucidate the formation mechanisms of semiconductor NCs.[7] However, the formation mechanism of nonfluorescent NCs such as iron oxide NCs is extremely difficult to study because there are no readily available tools to acquire size data for these oxide NCs. In particular, the sizes of oxide NCs that are smaller than 2 nm are hard to determine accurately.

Various mass spectrometry (MS) methods have been employed to characterize nanoclusters and small-sized NCs.[10] Most of the MS characterizations have focused on gold clusters, and there are only a few reports on oxide NCs with sizes of a few nanometers. Herein we report on the accurate characterization of sizes and size distributions of <5 nm iron oxide NCs using MS. Furthermore, we were able to use this MS-based technique to investigate the formation mechanism of extremely small iron oxide NCs. Among the various MS techniques, matrix-assisted laser desorption/ionization time of flight (MALDI-TOF) MS was employed because the use of a matrix in the MALDI technique keeps the NCs intact from fragmentation during the ionization step and the TOF analyzer can theoretically cover an infinite range of masses.[11a]

Received: October 10, 2012
Published: January 28, 2013

   dx.doi.org/10.1021/ja310030c | J. Am. Chem. Soc. 2013, 135, 2407−2410

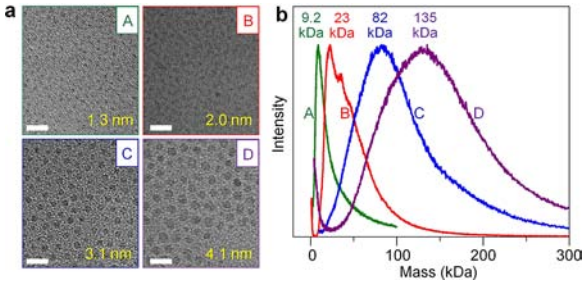

Figure 1. (a) TEM images of 1 nm (green; A), 2 nm (red; B), 3 nm (blue; C), and 4 nm (violet; D) iron oxide NCs. The scale bar is 10 nm. (b) MALDI-TOF mass spectra of iron oxide NCs shown in (a).

Iron oxide NCs with approximate sizes of 1, 2, 3, and 4 nm (Figure 1a) were synthesized by the thermal decomposition of iron−oleate complexes via the heat-up process.[5] The Fourier transform IR (FT-IR) spectrum of the NCs after the washing process showed a very weak peak at 1710 cm^{-1} and strong peaks at 1558 and 1444 cm^{-1} [Figure S1 in the Supporting Information (SI)], demonstrating that almost all of the free oleic acid was removed and that oleate was strongly bound to the NC surface.[11b]

XRD patterns of the NCs showed the ferrite structure (Figure S2a). Previous reports revealed that <4 nm iron oxide NCs have the maghemite structure.[4a,b] UV−vis spectra showed no size-dependent optical properties (Figure S2b). The magnetic properties of the iron oxide NCs changed dramatically according to their size. Nanocrystals with sizes of ≤2 nm exhibited nearly paramagnetic behavior, whereas the 3 and 4 nm-sized NCs were weakly superparamagnetic (Figure S3).

To obtain highly resolved mass spectra of iron oxide NCs, it is important to select an appropriate matrix. Aromatic carboxylic acids, which are the most popular matrixes for MALDI-TOF MS, are inappropriate for the desorption and ionization of iron oxide NCs because of their reactivity with iron oxide. Instead, nonacidic 9-nitroanthracene (9-NA) was used as the matrix. This enabled the generation of intact ions of iron oxide NCs as a result of 9-NA's minimal interaction and excellent miscibility with the hydrophobic NCs. Using 9-NA as a matrix, we successfully obtained MALDI-TOF mass spectra with peak positions at 9.2, 23, 82, and 135 kDa for 1, 2, 3, and 4 nm-sized NCs, respectively.

Since a single NC consists of both an inorganic core and a surfactant consisting of organic ligands, its total mass M can be written as the sum of the masses of the core and ligand portions ($M = M_{core} + M_{ligand}$). To determine the size of the inorganic core, the core mass fraction ($f = M_{core}/M$) was measured by thermogravimetric analysis (TGA) (Figure S4). The ratio of the sample masses before and after heating was taken as the f value because the organic surfactant was assumed to be totally removed by heating at 600 °C in air.[12] From the value of M obtained directly from the MALDI-TOF spectrum, the diameter D of the spherical particles was calculated as

$$D = \sqrt[3]{\frac{6Mf}{\rho N_A \pi}} \quad (1)$$

where ρ is the density of the core (4.87×10^{-21} g nm^{-3} for maghemite)[13] and N_A is Avogadro's number (mol^{-1} = Da g^{-1}). Since the core mass fraction of the 9.2 kDa NCs was 0.35, the particle size calculated using eq 1 was 1.28 nm (Figure 1b). This value is very close to the mean size of 1.27 ± 0.22 nm obtained from the TEM image (Figure 1a). The diameters of the 23, 82, and 135 kDa NCs were calculated to be 1.96, 3.28, and 3.91 nm, respectively, which also matched well with the corresponding values from the TEM images (1.97 ± 0.37, 3.05 ± 0.63, and 4.13

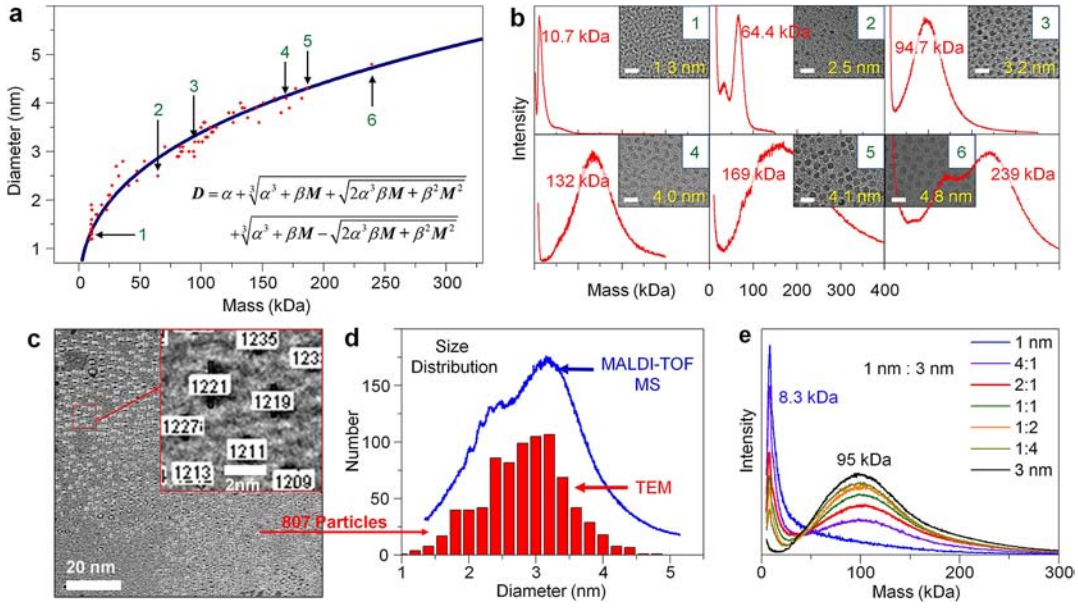

Figure 2. (a) The solid blue curve indicates the mass-diameter relationship from eq 2. The position of each red dot represents the MS peak position (x axis) and the mean diameter measured from TEM image (y axis) for iron oxide NCs synthesized from a single batch. There are 70 data points in the plot, which correspond to 70 batches of NCs with various sizes. (b) Six representative MS and TEM data sets used in (a). The corresponding data points in (a) are designated with arrows and numbers. The yellow numbers are the mean sizes from TEM images. Scale bars are 10 nm. (c) Counting 3 nm-sized iron oxide NCs in a TEM image for measuring the size distribution using Image J software (NIH). (d) Size distributions of iron oxide NCs measured from the TEM image in (c) (red bars) and obtained from the mass spectrum of the same NC sample using eq 2 (blue line). (e) MALDI-TOF mass spectra of 1 and 3 nm-sized iron oxide NCs and their 4:1, 2:1, 1:1, 1:2, and 1:4 mixtures.

dx.doi.org/10.1021/ja310030c | J. Am. Chem. Soc. 2013, 135, 2407−2410

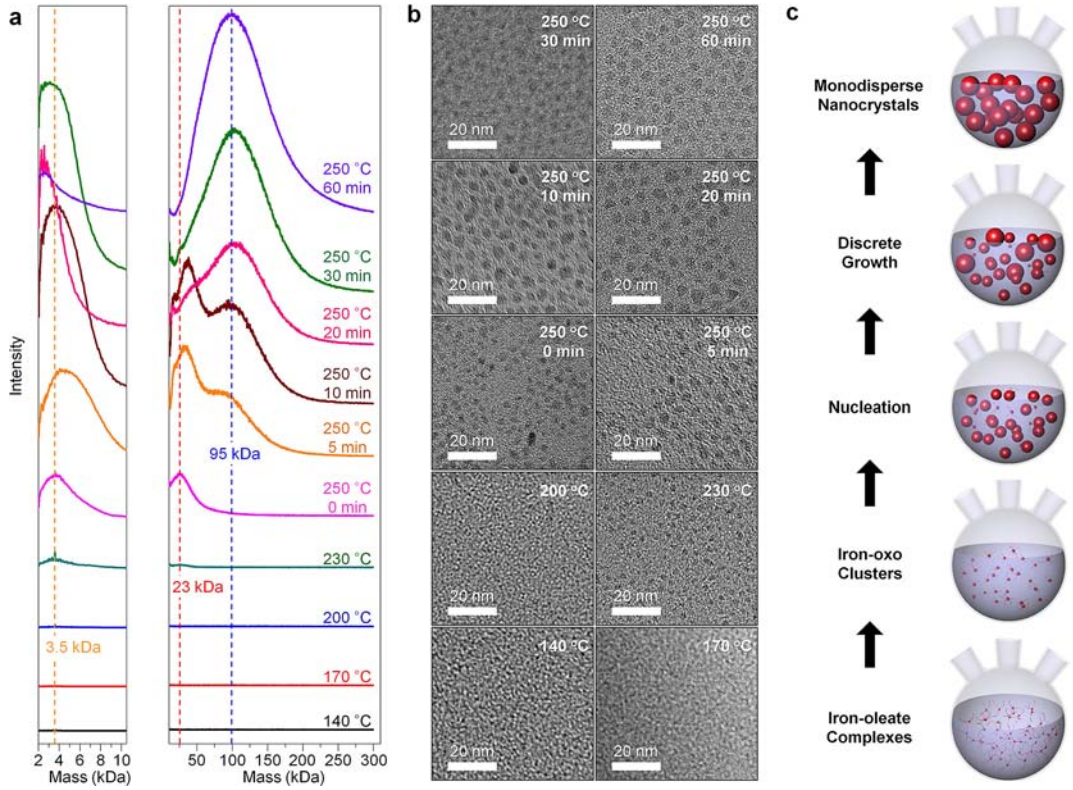

Figure 3. (a) Mass spectra of sample aliquots drawn from the reaction solution during heating. For clarity, the spectra in the mass ranges of <10.5 kDa (left) and >11 kDa (right) have been plotted using different scales. (b) TEM images of the NCs in the sample aliquots. (c) Schematics describing the formation mechanism proposed on the basis of the ex situ MS measurements.

nm ± 0.70 nm, respectively; Figure 1). Using MALDI-TOF mass spectrometry, we also measured the subnanometer-sized clusters (Figure S5).

If it is assumed that the packing density of the ligands on the NC surface (σ) is constant (Figure S6), then according to eq 1, f is a function of D. Thus, M values can be directly converted to values of D as follows:

$$D = \alpha + \sqrt[3]{\alpha^3 + \beta M + \sqrt{2\alpha^3\beta M + \beta^2 M^2}} + \sqrt[3]{\alpha^3 + \beta M - \sqrt{2\alpha^3\beta M + \beta^2 M^2}} \quad (2)$$

where $\alpha = -2\sigma m/\rho N_A \approx -0.754$ nm and $\beta = 3/\rho N_A \pi \approx 3.25 \times 10^{-4}$ nm^3 Da^{-1} (for the derivation of eq 2, see the SI).[14] Mass-to-diameter conversion data calculated using eq 2 are provided in Table S1 in the SI. To obtain an empirical relationship between the mass and the size of the NCs, we prepared NCs of various sizes from 70 batches of different synthetic conditions. The masses were obtained from the peak positions in the MALDI-TOF mass spectra, and the mean sizes were measured using TEM. In Figure 2a, the mass and size data are plotted as red dots. The mass−diameter curve calculated with eq 2 (blue line in Figure 2a) gives an excellent description of the empirical data. All 70 data sets of mass spectra and TEM images for the NCs are provided in Figure S7 and Table S2, and six sets are shown in Figure 2b as examples.

The mass−size relationship can be utilized to determine the size distribution of the NCs in a quick and accurate way. We obtained the size distribution of iron oxide NCs by measuring 807 NCs on a TEM image (Figure 2c). On the other hand, the mass spectrum of the same NCs was directly converted to a size distribution using eq 2. As shown in Figure 2d, the size distributions obtained from the TEM image and the mass spectrum have a good resemblance. Mass spectra of polydisperse iron oxide NCs prepared by mixing 1 and 3 nm-sized nanoparticles at various ratios were also obtained (Figure S8). As the fraction of 1 nm-sized nanoparticles decreased, the 8.3 kDa peak (corresponding to a size of 1.2 nm as calculated by eq 2) continuously decreased simultaneously with a gradual increase in the 95 kDa peak (corresponding to 3.3 nm as calculated by eq 2) (Figure 2e). These results clearly demonstrate that MALDI-TOF MS can be used to characterize the size of polydisperse nanoparticles. Our results in Figures 1 and 2 clearly show that MS provides a powerful tool for fast and accurate determination of the NC size distribution with a resolution of a few angstroms.

Our MS-based size estimation method is very useful especially for the observation of extremely small NCs and clusters. Unlike semiconductor NCs, during the synthesis of metal oxide NCs, it is extremely difficult to monitor the transition from molecular precursors to NCs. Mass-to-size estimation using MALDI-TOF MS enables us to measure precisely any size changes in the range from subnanometer to a few nanometers, which should be unprecedentedly useful in mechanistic studies of NC formation. As a model study, we carried out ex situ measurements on the synthesis of extremely small 3 nm-sized iron oxide NCs. The reaction mixture was prepared using the iron−oleate complex as the precursor for iron oxide NCs.[5] It was heated to 250 °C at a rate of 10 °C min^{-1} and then kept at the same temperature for 60 min. During the heating procedure, a series of sample aliquots were drawn from the reaction solution and analyzed with MALDI-TOF MS and TEM (Figure 3a,b). At 230 °C, the first peak in the mass spectrum appeared at 3.5 kDa. According to ref 8, thermal decomposition of the iron−oleate complex starts at

dx.doi.org/10.1021/ja310030c | J. Am. Chem. Soc. 2013, 135, 2407−2410

~230 °C, forming iron−oxo clusters coordinated with oleate groups. A mass of 3.5 kDa is close to the mass of an iron−oxo cluster that consists of ~8 iron atoms coordinated with ~11 oleate molecules. Further heating to 250 °C resulted in the growth of another peak at 23 kDa which corresponds to 1.9 nm-sized iron oxide NCs. After the reaction mixture was aged for 5 min at 250 °C, a third peak appeared at 95 kDa, from which a NC size of 3.3 nm was calculated. Mass-to-size estimations from the mass spectra coincided with the size data from TEM (Figure 3b).

The MS data in Figure 3a give very important information concerning iron oxide NC formation. Actually, these data clearly show that iron−oleate precursors were transformed to clusters and then to the final NCs during heating. The increase in the 3.5 kDa peak intensity at temperatures higher than 230 °C indicates that clusters were produced from iron−oleate complexes and accumulated in the solution. At 250 °C, nucleation took place from those clusters, and some of the larger clusters grew into NCs that were detected at 23 kDa (1.9 nm).[15] During aging at 250 °C, those NCs grew further to 95 kDa (3.3 nm). After aging for 60 min, all of the NCs had grown to 3.3 nm, consuming almost all of the clusters, and there was only one peak at 95 kDa in the mass spectrum. Interestingly, the growth of NCs from 1.9 to 3.3 nm was not continuous (Figure 3c). Instead, it seems that the size of the NCs was shifted from small to large. We think that those 1.9 and 3.3 nm-sized NCs are so-called "magic-sized" NCs that have extra stability with thermodynamically favored structures.[14,15]

In conclusion, we have demonstrated that MALDI-TOF MS is a powerful technique for characterizing the sizes of <5 nm iron oxide nanocrystals. By combining the relationship between mass and size of NCs and empirical data, we devised a mass-to-size estimation method that enables accurate, reliable, and fast characterization of ultrasmall iron oxide NCs. We utilized this technique to monitor the formation process of 3 nm-sized iron oxide NCs. Ex situ measurements showed that the formation of iron−oxo clusters leads to the nucleation of iron oxide NCs and that NCs with sizes of only a few nanometers grow discretely from smaller to larger sizes. We expect that our mass-to-size estimation will prove to be an easy-to-use and accurate analytical tool for various purposes, including not only the characterization of the size-dependent properties of NCs but also the study of formation mechanisms to develop new synthetic methods for various kinds of NCs with desired characteristics.

■ ASSOCIATED CONTENT

Supporting Information

Detailed experimental procedures; derivation of eq 2; process for obtaining particle sizes from TEM images; complete ref 5; FT-IR, XRD, UV−vis, vibrating sample magnetometry, and TGA data for iron oxide NCs; correlation between D and f; and MALDI-TOF mass spectra and TEM images of 70 samples of ultrasmall-sized iron oxide NCs. This material is available free of charge via the Internet at http://pubs.acs.org.

■ AUTHOR INFORMATION

Corresponding Author

thyeon@snu.ac.kr

Notes

The authors declare no competing financial interest.

■ ACKNOWLEDGMENTS

T.H. acknowledges financial support by the Research Center Program of the Institute for Basic Science in Korea. We thank K. H. Lim of the National Center for Inter-University Research Facilities (NCIRF) for MALDI-TOF MS experiments.

■ REFERENCES

(1) (a) Murray, C. B.; Norris, D. J.; Bawendi, M. G. *J. Am. Chem. Soc.* **1993**, *115*, 8706. (b) Alivisatos, A. P. *Science* **1996**, *271*, 933. (c) Talapin, D. V.; Lee, J.-S.; Kovalenko, M. V.; Shevchenko, E. V. *Chem. Rev.* **2010**, *110*, 389. (d) Joo, S. H.; Park, J. Y.; Renzas, J. R.; Butcher, D. R.; Huang, W.; Somorjai, G. A. *Nano Lett.* **2010**, *10*, 2709.

(2) Wilcoxon, J. P.; Martin, J. E.; Provencio, P. *J. Chem. Phys.* **2001**, *115*, 998.

(3) (a) Cullity, B. D.; Stock, S. R. *Elements of X-ray Diffraction*, 3rd ed.; Prentice Hall: New York, 2001. (b) Grabs, I.-M.; Bradtmöller, C.; Menzel, D.; Garnweitner, G. *Cryst. Growth Des.* **2012**, *12*, 1499. (c) Saunders, A. E.; Sigman, M. B., Jr.; Korgel, B. A. *J. Phys. Chem. B* **2004**, *108*, 193.

(4) (a) Park, J.; An, K.; Hwang, Y.; Park, J.-G.; Noh, H.-J.; Kim, J.-Y.; Park, J.-H.; Hwang, N.-M.; Hyeon, T. *Nat. Mater.* **2004**, *3*, 891. (b) Park, J.; Lee, E.; Hwang, N.-M.; Kang, M.; Kim, S. C.; Hwang, Y.; Park, J.-G.; Noh, H.-J.; Kim, J.-Y.; Park, J.-H.; Hyeon, T. *Angew. Chem., Int. Ed.* **2005**, *44*, 2872. (c) Sun, S.; Zeng, H. *J. Am. Chem. Soc.* **2002**, *124*, 8204. (d) Jun, Y.-w.; Huh, Y.-M.; Choi, J.-s.; Lee, J.-H.; Song, H.-T.; Kim, S.; Yoon, S.; Kim, K.-S.; Shin, J.-S.; Suh, J.-S.; Cheon, J. *J. Am. Chem. Soc.* **2005**, *127*, 5732. (e) Lee, N.; Hyeon, T. *Chem. Soc. Rev.* **2012**, *41*, 2575.

(5) Kim, B. H.; et al. *J. Am. Chem. Soc.* **2011**, *133*, 12624.

(6) Gatteschi, D.; Fittipaldi, M.; Sangregorio, C.; Sorace, L. *Angew. Chem., Int. Ed.* **2012**, *51*, 4792.

(7) (a) Talapin, D. V.; Rogach, A. L.; Shevchenko, E. V.; Kornowski, A.; Haase, M.; Weller, H. *J. Am. Chem. Soc.* **2002**, *124*, 5782. (b) Peng, X.; Wickham, J.; Alivisatos, A. P. *J. Am. Chem. Soc.* **1998**, *120*, 5343. (c) Peng, Z. A.; Peng, X. *J. Am. Chem. Soc.* **2002**, *124*, 3343. (d) Kudera, S.; Zanella, M.; Giannini, C.; Rizzo, A.; Li, Y.; Gigli, G.; Cingolani, R.; Ciccarella, G.; Spahl, W.; Parak, W. J.; Manna, L. *Adv. Mater.* **2007**, *19*, 548.

(8) Kwon, S. G.; Piao, Y.; Park, J.; Angappane, S.; Jo, Y.; Hwang, N.-M.; Park, J.-G.; Hyeon, T. *J. Am. Chem. Soc.* **2007**, *129*, 12571.

(9) (a) Zheng, H.; Smith, R. K.; Jun, Y.-w.; Kisielowski, C.; Dahmen, U.; Alivisatos, A. P. *Science* **2009**, *324*, 1309. (b) Yuk, J. M.; Park, J.; Ercius, P.; Kim, K.; Hellebusch, D. J.; Crommie, M. F.; Lee, J. Y.; Zettl, A.; Alivisatos, A. P. *Science* **2012**, *336*, 61.

(10) (a) Khitrov, G. A.; Strouse, G. F. *J. Am. Chem. Soc.* **2003**, *125*, 10465. (b) Levi-Kalisman, Y.; Jadzinsky, P. D.; Kalisman, N.; Tsunoyama, H.; Tsukuda, T.; Bushnell, D. A.; Kornberg, R. D. *J. Am. Chem. Soc.* **2011**, *133*, 2976. (c) Whetten, R. L.; Khoury, J. T.; Alvarez, M. M.; Murthy, S.; Vezmar, I.; Wang, Z. L.; Stephens, P. W.; Cleveland, C. L.; Luedtke, W. D.; Landman, U. *Adv. Mater.* **1996**, *8*, 428. (d) Alvarez, M. M.; Khoury, J. T.; Schaaff, T. G.; Shafigullin, M. N.; Vezmar, I.; Whetten, R. L. *J. Phys. Chem. B* **1997**, *101*, 3706. (e) Dass, A.; Stevenson, A.; Dubay, G. R.; Tracy, J. B.; Murray, R. W. *J. Am. Chem. Soc.* **2008**, *130*, 5940.

(11) (a) Skoog, D. A.; Holler, F. J.; Nieman, T. A. *Principles of Instrumental Analysis*, 5th ed.; Harcourt College Publishers: Orlando, FL, 1998. (b) Wu, N.; Fu, L.; Su, M.; Aslam, M.; Wong, K. C.; Dravid, V. P. *Nano Lett.* **2004**, *4*, 383.

(12) Qian, H.; Zhu, Y.; Jin, R. *Proc. Natl. Acad. Sci. U.S.A.* **2012**, *109*, 696.

(13) Cornell, R. M.; Schwertmann, U. *The Iron Oxides: Structure, Properties, Reactions, Occurrences and Uses*, 2nd ed.; Wiley-VCH: Weinheim, Germany, 2003.

(14) Viali, W. R.; Alcantara, G. B.; Sartoratto, P. P. C.; Soler, M. A. G.; Mosiniewicz-Szablewska, E.; Andrzejewski, B.; Morais, P. C. *J. Phys. Chem. C* **2010**, *114*, 179.

(15) Sugimoto, T. *Monodispersed Particles*; Elsevier: New York, 2001.